




Review

Late Transition Metal Olefin Polymerization Catalysts Derived from 8-Arylnaphthylamines

Zonglin Qiu^{1,†}, Wenyan Wang^{2,†}, Handou Zheng^{1,*}, Dengfei Wang², Xinglong Zhao², Guangshui Tu¹, Jiahao Yang¹ and Haiyang Gao^{1,*}

¹ School of Materials Science and Engineering, PCFM Lab, GD HPPC Lab, Sun Yat-sen University, Guangzhou 510275, China; qiuZlin3@mail2.sysu.edu.cn (Z.Q.); tugsh@mail2.sysu.edu.cn (G.T.); yangjh73@mail2.sysu.edu.cn (J.Y.)

² Daqing Petrochemical Research Center, Petrochemical Research Institute of PetroChina, Daqing 163714, China; wwy459@petrochina.com.cn (W.W.); wdf459@petrochina.com.cn (D.W.); zhaoxl459@petrochina.com.cn (X.Z.)

* Correspondence: zhenghdou@mail.sysu.edu.cn (H.Z.); gaohy@mail.sysu.edu.cn (H.G.)

† These authors contributed equally to this work.

Abstract: Late transition metal catalysts represent a significant class of olefin polymerization catalysts that have played an essential role in advancing the polyolefin industry owing to their highly tunable ligands and low oxophilicity. A key feature for the design of late transition metal catalysts lies in the steric bulk of the *o*-aryl substituents. Bulky 8-arylnaphthylamines have emerged as a promising aniline candidate for conducting high-performance catalysts by introducing axially steric hindrance around the metal center. This review focuses on late transition metal (Ni, Pd, Fe) catalysts derived from 8-arylnaphthylamines, surveying their synthesis, structural features, and catalytic applications in olefin (co)polymerizations. Additionally, the relationship between catalyst structure and catalytic performance is discussed, highlighting how these unique ligand systems influence polymerization activity, molecular weight, and polymer branching.

Keywords: late transition metal catalyst; N donor; steric effect; ethylene; catalytic polymerization



Citation: Qiu, Z.; Wang, W.; Zheng, H.; Wang, D.; Zhao, X.; Tu, G.; Yang, J.; Gao, H. Late Transition Metal Olefin Polymerization Catalysts Derived from 8-Arylnaphthylamines. *Inorganics* **2024**, *12*, 277. <https://doi.org/10.3390/inorganics12110277>

Academic Editor: László Kótai

Received: 30 September 2024

Revised: 24 October 2024

Accepted: 26 October 2024

Published: 28 October 2024



Copyright: © 2024 by the authors. Licensee MDPI, Basel, Switzerland. This article is an open access article distributed under the terms and conditions of the Creative Commons Attribution (CC BY) license (<https://creativecommons.org/licenses/by/4.0/>).

1. Introduction

Olefin polymerization catalysts have played a dominant role in the development of the polyolefin industry, driving advancements in both materials and industrial processes [1,2]. In particular, late transition metal catalysts have facilitated significant breakthroughs in the synthesis of high-performance functional polyolefins with varied structures and functionalities due to the low oxophilicity of their metal centers and the easily tunable ligands [3–6]. Late transition metal catalysts are often formed by the activation of the main catalysts (late transition metal complexes) by cocatalysts (e.g., alkylaluminum compounds), which can initiate olefins polymerization. Late transition metal complexes are typically composed of ligands and late transition metals such as nickel (Ni), palladium (Pd), iron (Fe), and cobalt (Co). Ligand diversity makes these catalyst systems versatile for a range of olefin polymerizations [7]. Usually, ligands feature nitrogen donor atoms as primary ligating groups, although oxygen and phosphorus donors are also commonly employed [8–17].

Historically, late transition metal nickel catalysts were primarily employed for ethylene oligomerization in the early stages because of rapid chain transfer via β -H elimination [18]. However, a significant breakthrough occurred in 1995 when Brookhart discovered the α -diimine nickel and palladium catalysts [19]. These catalysts featured bulky *ortho*-isopropyl substituents on the aryl moieties of the α -diimine ligands, increasing steric hindrance around the metal center. This modification effectively shielded the axial coordination sites, significantly suppressing the chain transfer process (associative displacement or chain transfer to bound monomer) and enabling the synthesis of high molecular weight polyolefins [19,20].

Since the discovery of α -diimine nickel and palladium catalyst systems, extensive research has focused on further modifying the ligand structure to enhance catalyst performance [21]. A key strategy has been the introduction of bulky *ortho*-aryl substituents on the aryl moiety, including phenyl [22,23], 2,6-diarylylhydyl [24–26], pentiptycenylyl [27–29], and the particularly unique 8-arylnaphthyl substituents [30,31] (Figure 1). The 8-arylnaphthylamines are known for creating a “sandwich-like” structure around the metal center, and their use has gained significant attention because the bulky 8-arylnaphthylamines provide a unique chemical environment around the metal center, which is not realized by other aniline compounds [30,31].

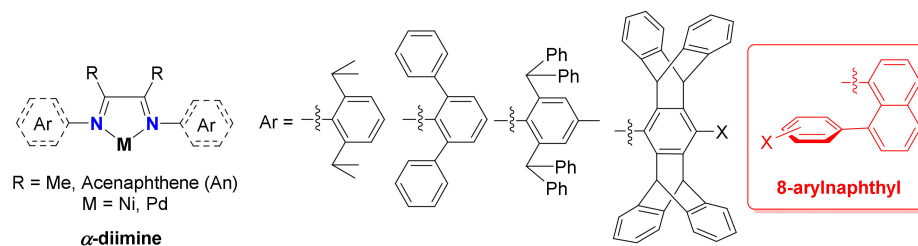


Figure 1. α -Diimine nickel and palladium catalysts with different *ortho*-aryl substituents.

Considering unique axially steric hindrance, 8-arylnaphthyl substituents have also been introduced into late transition metal catalysts with other chelate ligands, including pyridine-imine, bis(imino)pyridyl, salicylaldimine, and α -imino-ketone ligands (Figure 2) [9,32]. Catalysts featuring these various 8-arylnaphthyl substituted ligands have shown promise in olefin polymerizations and offer new pathways for tuning catalytic performance and polymer properties. In this review, we primarily survey the synthesis and structural characteristics of late transition metal catalysts featuring 8-arylnaphthyl substituents and their catalytic applications in olefin (co)polymerizations. The relationship between catalyst structure and catalytic performance will also be discussed, providing valuable insights for the future design of high-performance olefin polymerization catalysts.

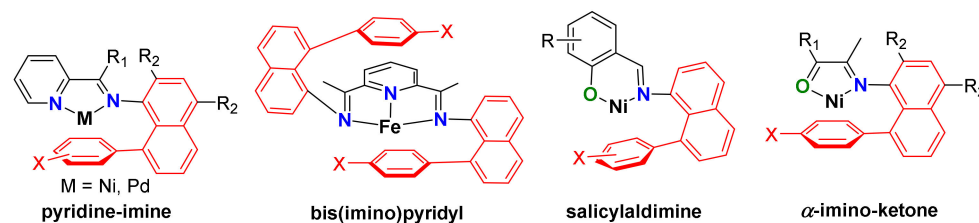
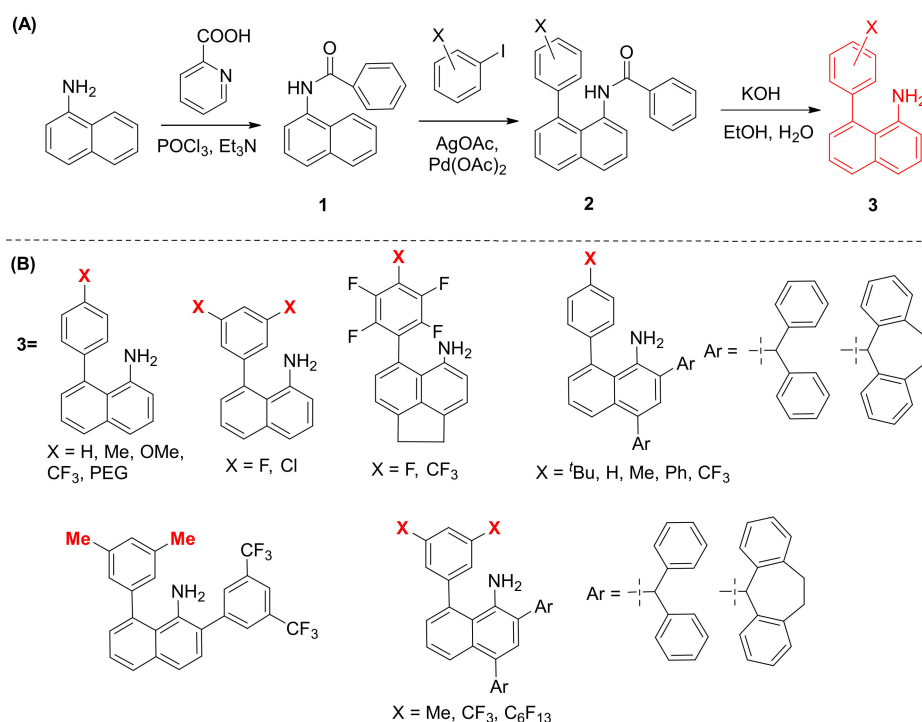


Figure 2. Late transition metal catalysts with 8-arylnaphthyl substituents.

2. Synthesis of 8-Arylnaphthylamines

The 8-arylnaphthylamine compound **3** can be synthesized through the synthetic route shown in Scheme 1A [33,34]. *N*-(naphthalen-1-yl)picolinamide **1** is generated by the reaction of 1-naphthylamine and picolinic acid. The C-H bond functionalization reaction requires Pd(OAc)₂ as a catalyst and stoichiometric AgOAc for halide removal and proceeds in the absence of solvent to yield *N*-(8-arylnaphthalen-1-yl)picolinamide **2**. The hydrolysis of amide **2** results in the formation of 8-arylnaphthylamine. Each step of the synthesis demonstrates high yields, and the resulting amine is purified following chromatography. The resulting amines can be further modified through coupling reactions to obtain aromatic amines with substituents (X) exhibiting varying steric and electronic effects (Scheme 1B) [35]. The obtained 8-(X-phenyl)naphthylamines can be used to synthesize various ligands through condensation reactions.



Scheme 1. Synthetic route of 8-arylnaphthylamines (A) and the corresponding 8-(X-phenyl)naphthylamines (B).

3. α -Diimine Nickel and Palladium Catalysts

Brookhart and coworkers first synthesized “sandwich-like” α -diimine nickel complexes **4** (Figure 3) in 2013 [30]. The single crystal structures of these complexes show a smaller distorted tetrahedral geometry around the nickel center compared with traditional dihalide-nickel complexes [36–39], which is attributed to the axial 8-arylnaphthyl substituents. The bulky 8-arylnaphthyl substituents are oriented perpendicular to the naphthyl planes and shield the axial up and down sites of the metal center, effectively suppressing chain transfer processes. Consequently, catalysts featuring 8-arylnaphthylamines have demonstrated the ability to produce high molecular weight polyolefin. After activation with modified methylalumoxane (MMAO), these “sandwich-like” nickel catalysts were able to catalyze ethylene polymerization, producing high molecular weight ($M_n > 10^6$ g/mol) and highly branched (up to 85/1000C) polyethylene (PE) (Entry 1 and 2 in Table 1). However, turnover frequencies (TOFs) indicated that the polymerization activity of these nickel catalysts was lower than that of nickel catalysts with *ortho*-isopropyl substituents (TOF: 1.4×10^5 vs. 8.5×10^5 mol PE/(mol Ni·h)), but the branching density of the obtained PE was significantly higher (85 vs. 60/1000C). The corresponding “sandwich-like” palladium complexes were also synthesized [31]. The single crystal structures of these palladium complexes exhibit square planar geometries around the palladium center, and the two tolyl rings also effectively cap the axial sites of the metal. These palladium complexes were further treated with acetonitrile and sodium tetrakis (3,5-bis(trifluoromethyl)phenyl)borate (NaBArF) to yield cationic palladium catalysts **5** (Figure 3). The cationic palladium catalysts can directly catalyze ethylene polymerization to yield more highly branched PEs (up to 117/1000C) compared with the corresponding nickel system in a living polymerization fashion (Entry 3 and 4 in Table 1). Additionally, palladium catalysts **5** achieved the copolymerization of ethylene (E) and methyl acrylate (MA), which exhibited decreased activity compared with traditional palladium catalysts. However, under the same conditions, the molecular weight and MA incorporation of the resulting EMA copolymer were higher. Overall, palladium catalysts **5** produced highly branched EMA copolymers with both high molecular weight and MA incorporation (up to 14%) (Entry 1 in Table 2).

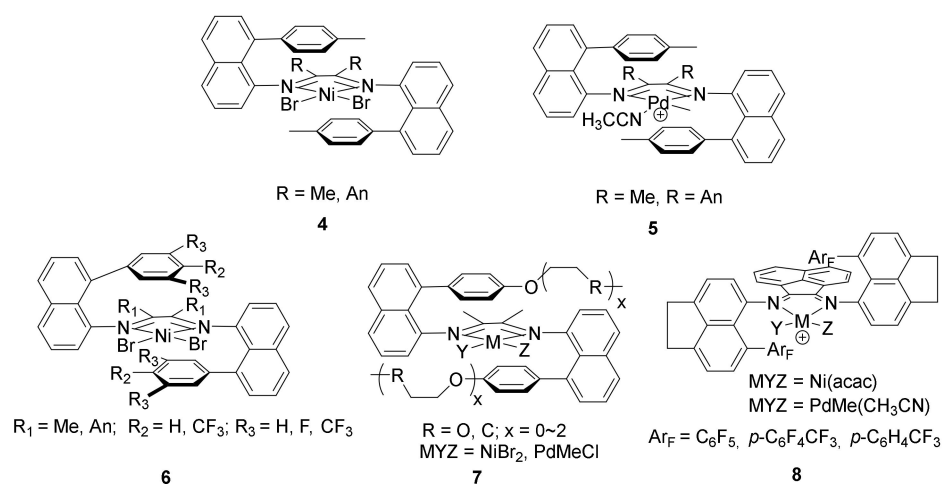


Figure 3. “Sandwich-like” α -Diimine nickel complexes with different substituents.

Coates and coworkers introduced fluorine and trifluoromethyl substituents on the “sandwich-like” ligand to form fluorinated nickel complexes **6** (Figure 3) [40–43]. The presence of these electron-withdrawing groups made the corresponding ligand synthesis more challenging and led to lower yields. In the presence of the cocatalyst methylaluminumoxane (MAO), catalysts **6** with trifluoromethyl substituents were able to catalyze the “chain-walking” polymerization of α -olefins, producing semicrystalline polyethylene-type materials with distinct melting temperatures ($T_m > 100$ °C) (Entry 1 in Table 3) [40]. Moreover, catalysts **6** with fluorine substituents resulted in a switchable catalyst for ethylene polymerization in a living fashion and produced a well-defined tetrablock copolymer comprising both branched and highly linear PEs by varying polymerization temperatures and ethylene pressures (Entry 5 in Table 1) [43].

Jian reported a series of “sandwich-like” α -diimine nickel and palladium catalysts **7** with polyethylene glycol (PEG) units (Figure 3) [44]. The aryl rings with the PEG unit arms are sited perpendicular to the naphthyl planes, capping the metal center from two axial directions. However, the distances between the oxygen atoms in the PEG chains and the nickel center (>5.5 Å) and the palladium center (>5.1 Å) were far beyond the range of van der Waals radii of the oxygen atom and the nickel atom (3.55 Å) and the palladium atom (3.6 Å), suggesting that no weak interactions exist between the ligand and the metal centers [45]. However, the probable “ligand–cocatalyst effect” via the chelation of the oxygen atom in polyethylene glycol units with the aluminum atom in the activator was proposed as a unique secondary coordination interaction. The nickel catalysts **7** with varying polyethylene glycol units under the activation of an alkyl aluminum reagent drastically enhanced ethylene polymerization activities (~ 9 times) and notably demonstrated the ability to tune the branching densities of the resulting PEs (ranging from 19 to 106/1000C) (Entry 6 in Table 1). However, the corresponding palladium catalysts did not exhibit any activity for ethylene polymerization.

Recently, Brookhart and Daugulis reported a new series of “sandwich-like” nickel and palladium complexes **8** with perfluorinated aryl caps (Figure 3) [46]. Due to difficulties in introducing polyfluorinated aryl groups, the preparation of ligands follows procedures that are different from those for nonfluorinated sandwich catalysts, but these nickel and palladium complexes are all air stable. The single crystal structures of these complexes showed that the perfluorinated aryl caps were precisely centered over the nickel and palladium centers, with the distances between the *ipso*-carbons on the fluorinated caps and the palladium center (3.31 and 3.42 Å), as well as the nickel center (3.15 and 3.20 Å), being notably close. As a result, this led to higher steric hindrance around the metal centers compared with their nonfluorinated analogs. Polymer molecular weights can be controlled via hydrogen addition (hydrogenolysis) in these palladium-catalyzed systems (Entry 7 in Table 1), which is unusual for late-transition-metal-catalyzed olefin polymerizations

Table 1. Cont.

Entry	Catalyst	T (°C)	P (atm)	Time (h)	Act. ^b	M _n (10 ⁵ g/mol)	PDI	BD (/1000C)	T _m (°C)	Ref.
5 ^e	6 (R = F)	−35	6	0.17	0.6	0.1	1.2	9	128	[43]
6 ^f	7 (R = O, x = 2)	25	7.9	0.5	27.0	4.2	1.6	19	107	[44]
7 ^g	8 (Ar _F = 4-CF ₃ C ₆ F ₄)	25	17.6	16	0.1	1.0	1.2	123	− ^d	[46]
8 ^h	8 (Ar _F = 4-CF ₃ C ₆ F ₄)	25	13.6	0.17	225.9	63	1.1	30	104	[46]
9 ⁱ	9 (X = Me)	80	10	0.5	6.3	1.7	1.6	36	85	[47]
10 ⁱ	10 (X = Me)	80	10	0.5	5.6	1.9	1.8	39	83	[47]
11 ^j	12 (R ₁ = <i>p</i> -Tol)	30	5	0.5	4.8	4.4	1.26	168	− ^d	[51]

^a Conditions: 1.6 μmol of Ni, MMAO, Al/Ni = 1000, toluene 200 mL; ^b Activity in 10⁵ g mol^{−1} h^{−1}; ^c 10 μmol of Pd, CH₂Cl₂ 40 mL; ^d Not determined; ^e 5 μmol of Ni, Et₂AlCl, Al/Ni = 300, toluene 100 mL; ^f 2 μmol of Ni, MMAO, Al/Ni = 1000, toluene/CH₂Cl₂ (48/2 mL); ^g 10 μmol of Pd, CH₂Cl₂ 50 mL, [H₂] 0.3 atm; ^h 0.5 μmol of Ni, Et₂AlCl, Al/Ni = 1000, toluene/CH₂Cl₂ (150/2 mL); ⁱ 2 μmol of Ni, Et₂AlCl, Al/Ni = 600, toluene/CH₂Cl₂ (48/2 mL); ^j 2 μmol of Ni, MAO, Al/Ni = 500, toluene/CH₂Cl₂ (20/1 mL).

Table 2. Representative data for copolymerization of ethylene and MA with nickel and palladium catalysts.

Entry	Catalyst	T (°C)	P (atm)	Conc. (mol/L)	Time (h)	Act. ^a	M _n (10 ⁴ g/mol)	PDI	BD (/1000C)	X ^b (%)	T _m (°C)	Ref.
1 ^c	5 (R = Me)	25	6	5.0	16.5	0.6	0.5	1.5	121	13.8	− ^d	[31]
2 ^e	9 (X = Me)	80	10	2.0	6	1.2	0.6	1.9	35	2.9	97	[48]
3 ^f	12 (R ₁ = <i>p</i> -Tol)	30	4	2.0	12	1.1	1.0	1.3	120	3.9	− ^d	[51]
4 ^g	15 (R = OMe)	40	4	2.0	10	0.6	0.6	1.2	134	22.7	− ^d	[52]
5 ^g	16	40	4	2.0	10	0.9	1.3	1.4	121	15.3	− ^d	[53]

^a Activity in 10³ g mol^{−1} h^{−1}; ^b Incorporation of MA determined by ¹H NMR spectroscopy; ^c Conditions: 10 μmol of Pd, 0.05 mmol galvinoxyl, CH₂Cl₂ and MA 45 mL; ^d Not determined; ^e 5 μmol of Ni, MAO, Al/Ni = 200, toluene/chlorobenzene (37/2 mL); ^f 10 μmol of Pd, CH₂Cl₂ and MA 20 mL; ^g 20 μmol of Pd, CH₂Cl₂ and MA 20 mL.

Although the 8-arylnaphthyl substituents provide exceptionally effective axial shielding, they may suffer from reduced catalytic activity due to their bulky steric hindrance. The asymmetric substituents approach for the catalyst design may help to solve this problem. Building on this strategy, Dai and coworkers synthesized a series of asymmetric nickel and palladium complexes **12**, which simultaneously feature a bulky 8-arylnaphthyl group and a low steric hindrance aliphatic imine moiety (Figure 5) [51,54]. However, the synthesis of ligands containing aliphatic imine moieties is more challenging due to the poor stability of aliphatic imines, which are easy to decompose during purification processes. These palladium complexes were confirmed by ¹H and ¹³C NMR analyses to be a mixture of two isomers with different ratios due to the asymmetry of the ligands. According to the single crystal analysis, both nickel and palladium complexes showed “half sandwich-like” structures. For the “half-sandwich-like” α-diimine nickel and palladium catalysts, the 8-arylnaphthyl substituent is also effective in suppressing chain transfer and facilitating chain walking to obtain high molecular weight PEs and copolymers with highly branched structures (up to 168/1000C) (Entry 11 in Table 1 and Entry 3 in Table 2).

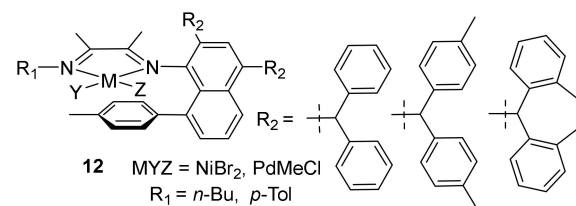


Figure 5. “Half-sandwich-like” α-diimine nickel and palladium catalysts.

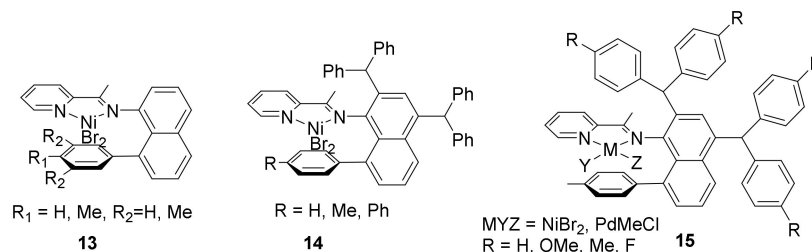
Table 3. Representative data for polymerization of α -olefins with nickel and palladium catalysts ^a.

Entry	Catalyst	Monomer	Conc. (mol/L)	Act. ^b	M_n (10^4 g/mol)	PDI	BD (/1000C)	T_m ($^{\circ}$ C)	Ref.
1 ^c	6 (R = CF ₃)	1-decene	0.1	0.5	3.2	1.2	- ^d	106	[40]
2 ^e	11	1-hexene	5.0	1.0	0.9	1.6	44	106	[50]
3 ^f	14 (R = Ph)	1-decene	0.1	0.2	1.3	1.5	26	105	[55]

^a Conditions: 24 h, 22 $^{\circ}$ C; ^b Activity in 10^3 g mol⁻¹ h⁻¹; ^c 5 μ mol of Ni, MAO, Al/Ni = 200, toluene/chlorobenzene (37/2 mL); ^d Not determined; ^e 5 μ mol of Pd, CH₂Cl₂ 25 mL; ^f 10 μ mol of Ni, Et₂AlCl, Al/Ni = 200, 2 mL CHCl₃, total volume 20 mL, 20 $^{\circ}$ C.

4. Pyridine-Imine Nickel and Palladium Catalysts

Pyridine-imine, as another type of [N,N] ligand, has also found numerous applications in late transition metal catalysts. Compared with the asymmetric “half sandwich-like” α -diimine ligand, the pyridine-imine ligands exhibit superior reactivity, ease of preparation, and enhanced chemical stability. Brookhart and Daugulis first synthesized the “half sandwich-like” pyridine-imine nickel complexes **13** (Figure 6) [56]. The single crystal structures of these nickel complexes show that these nickel complexes with smaller steric hindrances crystallize as centrosymmetric dimers in which each nickel atom is coordinated to a pyridine-imine ligand and two bridging halogen atoms. A terminal halide ion completes the square cone coordination layer. The phenyl substituents on the naphthyl moiety are nearly parallel to the five-membered chelate ring, effectively blocking an axial coordination site in the formation of mononuclear cationic complexes. When MMAO is used as a cocatalyst, these nickel catalysts **13** can catalyze ethylene polymerization and produce higher molecular weight PEs (M_n up to 2.6×10^4 g/mol) compared with pyridine-imine catalysts bearing a single ortho-disubstituted aryl group (Entry 1 in Table 4) [56].

**Figure 6.** Unsymmetrical pyridine-imine nickel and palladium catalysts with different substituents.**Table 4.** Representative data for the ethylene polymerizations with iron, nickel, and palladium catalysts.

Entry	Catalyst	T ($^{\circ}$ C)	P (atm)	Time (h)	Act. ^a	M_n (10^5 g/mol)	PDI	BD (/1000C)	T_m ($^{\circ}$ C)	Ref.
1 ^b	13 (R ₁ = CH ₃)	25	27.2	1	12.3	0.3	1.8	48	85	[56]
2 ^c	16	30	6	0.5	3.4	2	1.9	87	-4	[57]
3 ^c	17	30	6	0.5	2.4	0.4	1.6	73	54	[58]
4 ^d	18 (X = CF ₃)	30	10	0.5	12.7	0.02	15.1	- ^e	124	[59]
5 ^f	20 (R = CF ₃)	50	40.8	0.5	9.5	12.6	2.4	6	130	[60]
6 ^g	21 (X = ^t Bu)	20	9	0.5	6.9	5.7	1.4	23	103	[61]
7 ^h	22 (R ₁ = R ₂ = CF ₃)	60	39.4	0.5	80.7	11.1	1.2	3.5	128	[62]
8 ⁱ	23	90	39.5	0.5	32.5	6.6	1.5	15	108	[63]
9 ^j	24	40	8	0.5	10.0	8.4	2.6	26	116	[64]
10 ^k	25	25	27.2	4	2.7	41	1.2	19	ND	[65]
11 ^l	26 (R = ^t Bu)	80	8	1	6.0	12.3	2.0	70	63.4	[66]

^a Activity in 10^5 g mol⁻¹ h⁻¹; ^b 5.4 μ mol of Ni, MMAO Al/Ni = 1000, toluene 200 mL; ^c 2 μ mol of Ni, Et₂AlCl, Al/Ni = 200, toluene/CH₂Cl₂ (20/1 mL); ^d 2.4 μ mol of Fe, MAO, Al/Ni = 1000, toluene/CH₂Cl₂ (68/2 mL); ^e Not determined; ^f 5 μ mol of Ni, toluene 200 mL; ^g 10 μ mol of Ni, 20 μ mol of Ni(COD)₂, toluene 50 mL; ^h 5 μ mol of Ni, THF 100 mL; ⁱ 3 μ mol of Ni, 1,4-dioxane 100 mL; ^j 1 μ mol of Ni, MAO, Al/Ni = 80, toluene/CH₂Cl₂ (18/2 mL); ^k 2 μ mol of Ni, toluene 50 mL, catalyst added as a CH₂Cl₂ solution; ^l 1 μ mol of Ni, toluene/CH₂Cl₂ (28/2 mL).

Chen developed a series of pyridine-imine nickel complexes **14** containing both the dibenzhydryl and the 8-arylnaphthyl substituents (Figure 6) [55]. Due to the instability of the nickel complexes, multiple attempts to determine their molecular structure were unsuccessful. However, X-ray diffraction analysis of the ligand revealed that the 8-arylnaphthyl substituents were expected to effectively block the axial position of the metal center. These pyridine-imine nickel catalysts **14** exhibited high thermal stability and were capable of catalyzing ethylene polymerization with high activity to produce ultra-high molecular weight polyethylenes. Additionally, these nickel catalysts also effectively catalyzed the polymerization of α -olefins, yielding polymers with obvious melting temperature (T_m up to 105.5 °C) through significant chain straightening through a combination of 2,1-monomer insertion and precision chain walking (Entry 3 in Table 3).

Furthermore, Dai synthesized a series of pyridine-imine nickel and palladium complexes **15** (Figure 6) with the electronic effect of remote non-conjugated substituents (H, OMe, Me, F) [52]. Due to the asymmetry of the ligands, the palladium complexes in **15** were mixtures of two isomers with different ratios. The aryl rings are positioned directly over the metal center, indicating an effective blockage and shielding the axial positions of the metal center. These nickel catalysts exhibited moderate activities and generated highly branched (57~90/1000 C) PEs with high molecular weights ($\sim 10^5$ g/mol) in ethylene polymerization. Compared to classical Brookhart-type α -diimine catalysts, these palladium catalysts showed great advantages in the copolymerization of ethylene with polar monomers and produced EMA copolymers with significantly higher MA incorporation (8.4~10.9 times higher) and higher molecular weights (Entry 4 in Table 2).

The pyridine-imine nickel and palladium catalysts **16** (Figure 7) bearing dibenzosuberyl groups and 8-arylnaphthyl substituents were synthesized [53,57]. The 8-arylnaphthyl substituents and the phenyl rings of the dibenzosuberyl substituents are both nearly parallel to the five-membered coordination plane, effectively blocking the axial coordination sites of the metal complexes and creating a highly congested environment around the metal center ($\sim 51\% V_{\text{Bur}}$). These nickel catalysts containing both 8-arylnaphthyl and dibenzosuberyl substituents produced higher molecular weight PEs with higher branching density compared to those derived from “half-sandwich” nickel catalysts containing 8-arylnaphthyl and diarylmethyl groups (Entry 2 in Table 4).

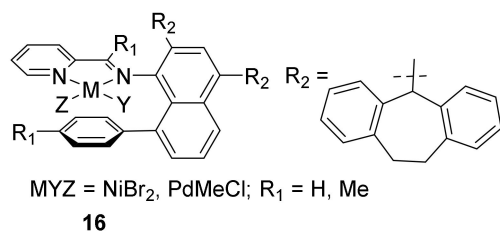


Figure 7. Unsymmetrical pyridine-imine nickel and palladium catalysts with dibenzosuberyl substituents.

These pyridine-imine palladium catalysts were highly efficient for the copolymerization of ethylene with various polar monomers, such as methyl acrylate (MA) (Entry 5 in Table 2), acrylic acid (AA), n-butyl acrylate (BA), and the fluorinated acrylate 2,2,3,4,4,4-hexafluorobutyl acrylate (6FA), enabling access to high-molecular-weight functionalized polyethylene (M_n up to 32 kg/mol) with high polar monomer incorporation (up to 24 mol%).

A series of pyridine-imine nickel and palladium complexes **17** with a flexible backbone were synthesized by Dai and coworkers (Figure 8) [58]. Although ¹H NMR analysis shows that the ligand with a flexible backbone has a certain proportion of enamine and imine interconversion isomers, these isomers are completely converted to imine structures during coordination with metal catalyst precursors. The nickel catalyst generated PEs with high branching densities (76/1000C) and high molecular weights (up to 35.3 kg/mol) (Entry 3 in Table 4). The palladium catalyst generated PEs similar to those of the nickel catalyst.

Moreover, highly branched (86~109/1000C) EMA copolymers with high molecular weights (up to 15.4 kg/mol) and high incorporation (up to 17.4 mol%) were achieved.

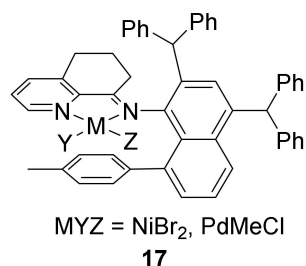


Figure 8. Pyridine-imine nickel and palladium catalysts with flexible backbone.

5. Bis(imino)pyridyl Iron Catalysts

Although the 8-arylnaphthylamine compounds are attractive anilines for the design of late transition metal Ni/Pd olefin polymerization catalysts, “sandwich” bis(imino)pyridyl iron catalysts had never been reported before our recent work [67–69], possibly because researchers are worried about their inactivity caused by bulky steric hindrance [70,71].

Our group synthesized a series of bis(imino)pyridyl iron complexes **18** (Figure 9) bearing substituted 8-(*p*-X-phenyl)naphthylamines (X = OMe, Me, H, CF₃) with different electron-donating/withdrawing groups [59]. The capping aryl substituents are positioned above and below and nearly parallel to the pyridyl ring. The buried volumes (%V_{Bur}) of **18** vary from 57.0 to 59.5. A buried volume of 59.5 for **18** (X = OMe) represents the largest value of the reported bis(imino)pyridyl iron complexes. Surprisingly, the existence of intramolecular π - π stacking interactions was clearly confirmed by single-crystal X-ray diffraction analysis, UV–vis, and photoluminescence spectra. Despite the bulky nature of our bis(imino)pyridyl iron catalysts, the intra-molecular π - π interactions cause the naphthyl rings to tilt away from the iron center in the horizontal direction. This results in a more open horizontal space within the iron complexes, facilitating ethylene coordination. Thus, ethylene polymerization results show that π - π interactions are a crucial driving force rather than the steric and electronic effects of ligands. Unprecedentedly, bulky “sandwich” bis(imino)pyridyl iron catalyst (X = CF₃) produces low-molecular-weight PE with a bimodal distribution (Entry 4 in Table 4). Two chain transfer pathways, including β -H transfer to ethylene monomer and chain transfer to aluminum, have been identified by clean separation of the two fractions. The β -H transfer to the ethylene monomer is the dominant chain transfer pathway in iron-catalyzed ethylene polymerization, which leads to a large proportion of low-molecular-weight unsaturated polyethylene. These unusual ethylene polymerization behaviors are ascribed to weak noncovalent π - π interactions.

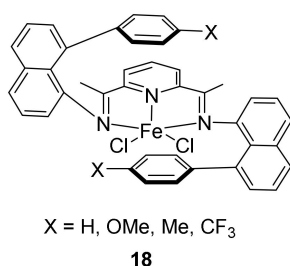


Figure 9. Bis(imino)pyridyl iron catalysts.

6. Salicylaldimine Nickel Catalysts

Brookhart and Daugulis reported the synthesis of neutral salicylaldimine nickel catalysts **19** and **20** (Figure 10) containing 8-arylnaphthyl substituents [60]. Unfortunately, nickel catalyst **19** derived from less sterically hindered amines could not be obtained due to its instability. The nickel catalysts **20** show high stability without decomposition over 2 weeks in a solvent. These nickel catalysts adopt a nearly square planar coordination geometry,

and the aryl rings effectively shield the axial sites above and below the square coordination plane. These active neutral nickel single-component catalysts generated lightly branched ultrahigh-molecular-weight polyethylene (UHMWPE) and showed a “quasi-living” polymerization behavior (Entry 5 in Table 4). Guo and Li prepared a series of salicylaldimine ligands with different substituents ($X = t\text{Bu}$, Me, H, CF_3) and the corresponding neutral salicylaldimine nickel complexes **21** (Figure 10) [61]. These nickel complexes exhibited high catalytic activity for ethylene polymerization ($6.88 \times 10^5 \text{ g}\cdot\text{mol}^{-1}\cdot\text{h}^{-1}$) (Entry 6 in Table 4), producing high molecular weight polyethylenes (up to $8.1 \times 10^5 \text{ g/mol}$).

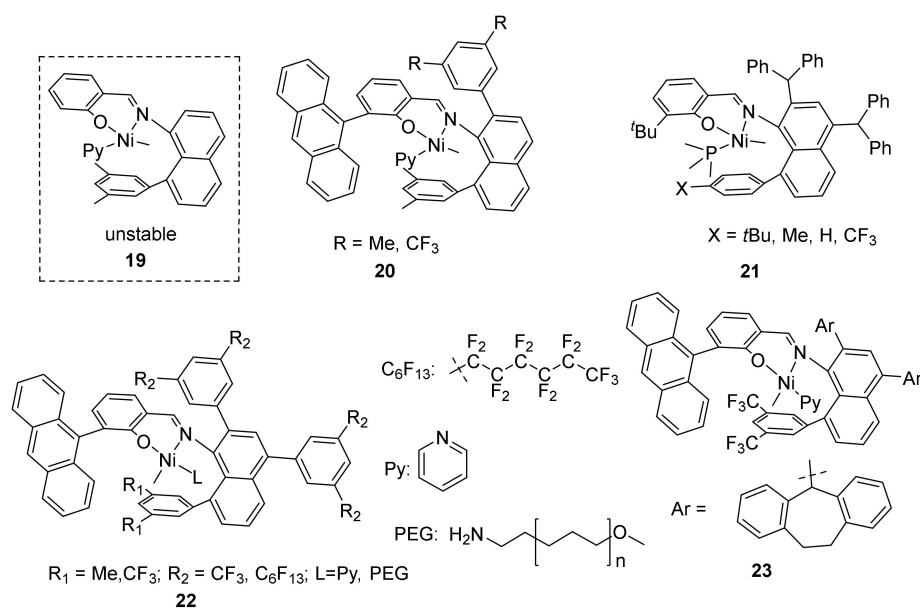


Figure 10. Salicylaldimine nickel catalysts with different substituents.

Mecking synthesized a series of neutral salicylaldimine nickel catalysts **22** (Figure 10) containing 8-arylnaphthyl substituents ($X =$ trifluoromethyl group and longer perfluoroalkyl groups) [62,72]. Unlike the previously performed multistep reaction based on C-H activation groups, naphthylamine derivatives were synthesized in a one-pot reaction, beginning with a selective, quantitative lithiation reaction, followed by the introduction of a boronic acid group. Suzuki coupling bromobenzene gave naphthylamine products in an 80% yield. These nickel catalysts exhibited enhanced activity and demonstrated living/controlled polymerization when using THF and diethyl ether as reaction media, allowing the production of ultra-high molecular weight polyethylene (UHMWPE) (Entry 7 in Table 4).

Jian and coworkers synthesized a neutral salicylaldimine nickel catalyst **23** (Figure 10) by the combination of 8-arylnaphthyl and dibenzosuberyl groups [63]. Verified by X-ray diffraction analysis, the aryl rings effectively shield the axial sites above and below the square coordination plane. Ethylene polymerization in a living fashion was achieved, enabling the production of virtually linear UHMWPE ($M_w = 6020 \text{ kg/mol}$). More importantly, catalyst **23** was able to produce UHMWPE ($M_w = 1002 \text{ kg/mol}$) even at elevated temperatures of up to $90 \text{ }^\circ\text{C}$ and in polar solvents (Entry 8 in Table 4).

7. Nickel and Palladium Catalysts Bearing Other [N,O] Chelate Ligands

Chen and coworkers developed a 2-iminopyridine-*N*-oxide ligand and the corresponding nickel catalyst **24** (Figure 11) by replacing the phenyl moiety of the salicylaldimine with a pyridyl moiety [64]. The nickel catalyst **24**, featuring diarylhydridyl and 8-arylnaphthyl substituents, was able to catalyze ethylene polymerization, producing high molecular weight polyethylene with low branch density (Entry 9 in Table 4). In addition, it could also catalyze the copolymerization with methyl 10-undecenoate.

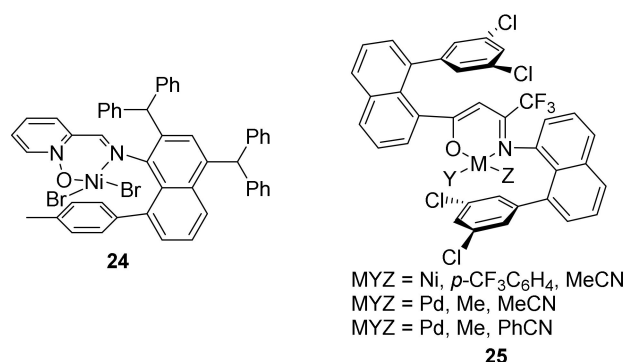


Figure 11. Nickel and palladium catalysts with other [N,O] chelate ligands.

Brookhart and Daugulis prepared a series of neutral β -ketoamine nickel and palladium catalysts **25** (Figure 11) [65]. The nickel complex was isolated as a mixture of two isomers in a 2.3:1 ratio after recrystallization and showed approximately square planar geometry at the nickel center. Efficient blocking of the nickel axial sites was characterized by X-ray crystallography. The arrangement of the aryl caps relative to the metal center is similar to that observed for the palladium complexes. In contrast to the nickel complex, these palladium complexes exist as single isomers in solution, and the nitrile ligand is positioned trans to the nitrogen in the solid state. The nickel catalyst produced lightly branched ultra-high molecular weight polyethylene (M_n up to 4.1×10^6 g/mol) (Entry 10 in Table 4), while the palladium catalysts generated relatively lower molecular weight polyethylene (only $\sim 10^4$ g/mol) with moderate branching ($\sim 50/1000C$).

Chen synthesized α -imino-ketone nickel catalysts **26** (Figure 12) bearing a combination of 8-arylnaphthyl and diarylmethyl groups [66]. The nickel center exhibited a square planar geometry, and these nickel catalysts were found to be diamagnetic. The sterically open configuration leaves one side of the nickel center fully exposed. These nickel catalysts produced branched ultra-high molecular weight PEs and also facilitated the copolymerization of ethylene with a series of polar comonomers (Entry 11 in Table 4).

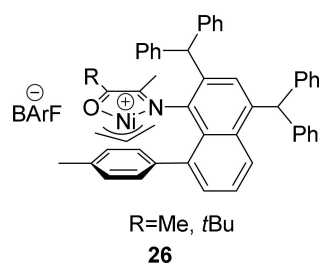


Figure 12. α -Imino-ketone nickel catalysts.

8. Conclusions and Outlook

The introduction of 8-arylnaphthylamines in late-transition metal catalysts represents a significant advancement in the field of olefin polymerization. These bulky ligands create “sandwich-like” or “half-sandwich-like” structures around the metal center, leading to increased steric hindrance and influencing both catalyst stability and reactivity. A variety of late transition metal (Ni, Pd, Fe) catalysts bearing 8-arylnaphthyl-based ligands, including α -diimine, pyridine-imine, bis(imino)pyridyl, salicylaldimine, and other [N,O] chelate ligands, have been explored for ethylene (co)polymerizations. Generally, the introduction of 8-arylnaphthylamines shields the axial sites of the metal center, effectively suppressing chain transfer and tuning the chain-walking processes. This allows for the production of high molecular weight polymers with finely tunable branching. However, we also note that the polymerization activity usually decreases because bulky steric hindrance prohibits the coordination of monomers. For these issues, further modification of the 8-arylnaphthylamines combining electronic effect substituents can enhance the per-

formance of the catalyst, particularly in terms of polymerization activity. For example, 8-halonaphthyl and 8-alkylnaphthyl Ni(II)/Pd(II) catalysts developed by Brookhart and Dai exhibit higher ethylene polymerization activity but produce bimodal-distribution PE because of equilibrating syn/anti catalyst diastereomers [73,74]. Based on a flexible axial shielding strategy, pyridine-imine Ni(II) and Pd(II) catalysts developed by Dai can synthesize high-molecular-weight PE and polar functionalized PE [75]. The continued development of novel ligand architectures incorporating 8-arylnaphthylamines holds significant promise for the design of next-generation catalysts in the polyolefin industry. Late transition metal olefin polymerization catalysts derived from 8-arylnaphthylamines would show significant potential for industrial applications, although they are currently employed in industrial production. Besides, copper catalysts featuring various 8-arylnaphthyl substituted α -diimine ligands also show improved performance in C-H functionalization [76–80], also showing great potential in catalytic small-molecule reactions.

Author Contributions: Writing—original draft preparation, Z.Q. and W.W.; writing—review, D.W., X.Z., G.T. and J.Y.; writing—review and editing, H.Z. and H.G.; funding acquisition, H.Z. and H.G. supervision, H.G. All authors have read and agreed to the published version of the manuscript.

Funding: This work was financially supported by National Natural Science Foundation of China (NSFC) (52173016), the State Key Research Development Program of China (Grant No. 2021YFB3800701), Guangdong Basic and Applied Basic Research Foundation (2024A1515012784, 2024A1515011102, and 2023A1515110549), Fundamental Research Funds for the Central Universities, Sun Yat-sen University (24qnp047), and PetroChina Projects (2022DJ6308, 2021DJ5902, and 2020-CB-02-13).

Conflicts of Interest: The authors declare no conflicts of interest.

References

- Galli, P.; Vecellio, G. Technology: Driving force behind innovation and growth of polyolefins. *Prog. Polym. Sci.* **2001**, *26*, 1287–1336. [[CrossRef](#)]
- Imanishi, Y.; Naga, N. Recent developments in olefin polymerizations with transition metal catalysts. *Prog. Polym. Sci.* **2001**, *26*, 1147–1198. [[CrossRef](#)]
- Berkefeld, A.; Mecking, S. Coordination copolymerization of polar vinyl monomers $H_2C=CHX$. *Angew. Chem. Int. Ed.* **2008**, *47*, 2538–2542. [[CrossRef](#)] [[PubMed](#)]
- Cheung, C.S.; Shi, X.; Pei, L.; Du, C.; Gao, H.; Qiu, Z.; Gao, H. Alternating copolymerization of carbon monoxide and vinyl arenes using [N,N] bidentate palladium catalysts. *J. Polym. Sci.* **2022**, *60*, 1448–1467. [[CrossRef](#)]
- Zheng, H.; Qiu, Z.; Li, D.; Pei, L.; Gao, H. Advance on nickel- and palladium-catalyzed insertion copolymerization of ethylene and acrylate monomers. *J. Polym. Sci.* **2023**, *61*, 2987–3021. [[CrossRef](#)]
- Xiao, X.; Zheng, H.; Gao, H.; Cheng, Z.; Feng, C.; Yang, J.; Gao, H. Recent advances in synthesis of non-alternating polyketone generated by copolymerization of carbon monoxide and ethylene. *Int. J. Mol. Sci.* **2024**, *25*, 1348. [[CrossRef](#)]
- Ittel, S.D.; Johnson, L.K.; Brookhart, M. Late-metal catalysts for ethylene homo- and copolymerization. *Chem. Rev.* **2000**, *100*, 1169–1204. [[CrossRef](#)]
- Mu, H.; Pan, L.; Song, D.; Li, Y. Neutral nickel catalysts for olefin homo- and copolymerization: Relationships between catalyst structures and catalytic properties. *Chem. Rev.* **2015**, *115*, 12091–12137. [[CrossRef](#)]
- Deng, H.; Zheng, H.; Gao, H.; Pei, L.; Gao, H. Late transition metal catalysts with chelating amines for olefin polymerization. *Catalysts* **2022**, *12*, 936. [[CrossRef](#)]
- Younkin, T.R.; Connor, E.F.; Henderson, J.I.; Friedrich, S.K.; Grubbs, R.H.; Bansleben, D.A. Neutral, single-component nickel (II) polyolefin catalysts that tolerate heteroatoms. *Science* **2000**, *287*, 460–462. [[CrossRef](#)]
- Wang, Z.; Liu, Q.; Solan, G.A.; Sun, W.-H. Recent advances in Ni-mediated ethylene chain growth: Nimine-donor ligand effects on catalytic activity, thermal stability and oligo-/polymer structure. *Coord. Chem. Rev.* **2017**, *350*, 68–83. [[CrossRef](#)]
- Zhong, L.; Li, G.; Liang, G.; Gao, H.; Wu, Q. Enhancing thermal stability and living fashion in α -diimine-nickel-catalyzed (co)polymerization of ethylene and polar monomer by increasing the steric bulk of ligand backbone. *Macromolecules* **2017**, *50*, 2675–2682. [[CrossRef](#)]
- Zhong, S.; Tan, Y.; Zhong, L.; Gao, J.; Liao, H.; Jiang, L.; Gao, H.; Wu, Q. Precision synthesis of ethylene and polar monomer copolymers by palladium-catalyzed living coordination copolymerization. *Macromolecules* **2017**, *50*, 5661–5669. [[CrossRef](#)]
- Zhong, L.; Du, C.; Liao, G.; Liao, H.; Zheng, H.; Wu, Q.; Gao, H. Effects of backbone substituent and intra-ligand hydrogen bonding interaction on ethylene polymerizations with alpha-diimine nickel catalysts. *J. Catal.* **2019**, *375*, 113–123. [[CrossRef](#)]
- Zhong, L.; Zheng, H.; Du, C.; Du, W.; Liao, G.; Cheung, C.S.; Gao, H. Thermally robust α -diimine nickel and palladium catalysts with constrained space for ethylene (co)polymerizations. *J. Catal.* **2020**, *384*, 208–217. [[CrossRef](#)]

16. Zheng, H.; Zhong, L.; Du, C.; Du, W.; Cheung, C.S.; Ruan, J.; Gao, H. Combining hydrogen bonding interactions with steric and electronic modifications for thermally robust α -diimine palladium catalysts toward ethylene (co)polymerization. *Catal. Sci. Technol.* **2021**, *11*, 124–135. [[CrossRef](#)]
17. Zheng, H.; Pei, L.; Deng, H.; Gao, H.; Gao, H. Electronic effects of amine-imine nickel and palladium catalysts on ethylene (co)polymerization. *Eur. Polym. J.* **2023**, *184*, 111773. [[CrossRef](#)]
18. Klabunde, U.; Itten, S.D. Nickel catalysis for ethylene homo- and co-polymerization. *J. Mol. Catal.* **1987**, *41*, 123–134. [[CrossRef](#)]
19. Johnson, L.K.; Killian, C.M.; Brookhart, M. New Pd(II)- and Ni(II)-based catalysts for polymerization of ethylene and α -olefins. *J. Am. Chem. Soc.* **1995**, *117*, 6414–6415. [[CrossRef](#)]
20. Johnson, L.K.; Mecking, S.; Brookhart, M. Copolymerization of ethylene and propylene with functionalized vinyl monomers by palladium(II) catalysts. *J. Am. Chem. Soc.* **1996**, *118*, 267–268. [[CrossRef](#)]
21. Wang, F.; Chen, C. A continuing legend: The Brookhart-type α -diimine nickel and palladium catalysts. *Polym. Chem.* **2019**, *10*, 2354–2369. [[CrossRef](#)]
22. Schmid, M.; Eberhardt, R.; Klinga, M.; Leskelä, M.; Rieger, B. New C_{2v} - and chiral C_2 -symmetric olefin polymerization catalysts based on nickel(II) and palladium(II) diimine complexes bearing 2,6-diphenyl aniline moieties: Synthesis, structural characterization, and first insight into polymerization properties. *Organometallics* **2001**, *20*, 2321–2330. [[CrossRef](#)]
23. Meinhard, D.; Wegner, M.; Kipiani, G.; Hearley, A.; Reuter, P.; Fischer, S.; Marti, O.; Rieger, B. New nickel(II) diimine complexes and the control of polyethylene microstructure by catalyst design. *J. Am. Chem. Soc.* **2007**, *129*, 9182–9191. [[CrossRef](#)] [[PubMed](#)]
24. Rhinehart, J.L.; Brown, L.A.; Long, B.K. A robust Ni(II) α -diimine catalyst for high temperature ethylene polymerization. *J. Am. Chem. Soc.* **2013**, *135*, 16316–16319. [[CrossRef](#)]
25. Rhinehart, J.L.; Mitchell, N.E.; Long, B.K. Enhancing α -diimine catalysts for high-temperature ethylene polymerization. *ACS Catal.* **2014**, *4*, 2501–2504. [[CrossRef](#)]
26. Dai, S.; Sui, X.; Chen, C. Highly robust palladium(II) α -diimine catalysts for slow-chain-walking polymerization of ethylene and copolymerization with methyl acrylate. *Angew. Chem. Int. Ed.* **2015**, *54*, 9948–9953. [[CrossRef](#)]
27. Kanai, Y.; Foro, S.; Plenio, H. Bispentiptycenyl-diimine-nickel complexes for ethene polymerization and copolymerization with polar monomers. *Organometallics* **2019**, *38*, 544–551. [[CrossRef](#)]
28. Liao, Y.D.; Zhang, Y.X.; Cui, L.; Mu, H.L.; Jian, Z.B. Pentiptycenylyl substituents in insertion polymerization with α -diimine nickel and palladium species. *Organometallics* **2019**, *38*, 2075–2083. [[CrossRef](#)]
29. Zhang, Y.; Wang, C.; Mecking, S.; Jian, Z. Ultrahigh branching of main-chain-functionalized polyethylenes by inverted insertion selectivity. *Angew. Chem. Int. Ed.* **2020**, *59*, 14296–14302. [[CrossRef](#)]
30. Zhang, D.; Nadres, E.T.; Brookhart, M.; Daugulis, O. Synthesis of highly branched polyethylene using “sandwich” (8-*p*-tolyl naphthyl α -diimine)nickel(II) catalysts. *Organometallics* **2013**, *32*, 5136–5143. [[CrossRef](#)]
31. Allen, K.E.; Campos, J.; Daugulis, O.; Brookhart, M. Living polymerization of ethylene and copolymerization of ethylene/methyl acrylate using “sandwich” diimine palladium catalysts. *ACS Catal.* **2015**, *5*, 456–464. [[CrossRef](#)]
32. Mu, H.; Zhou, G.; Hu, X.; Jian, Z. Recent advances in nickel mediated copolymerization of olefin with polar monomers. *Coord. Chem. Rev.* **2021**, *435*, 213802. [[CrossRef](#)]
33. Daugulis, O.; Zaitsev, V.G. Anilide *ortho*-arylation by using C–H activation methodology. *Angew. Chem. Int. Ed.* **2005**, *44*, 4046–4048. [[CrossRef](#)] [[PubMed](#)]
34. Zaitsev, V.G.; Shabashov, D.; Daugulis, O. Highly regioselective arylation of sp^3 C–H bonds catalyzed by palladium acetate. *J. Am. Chem. Soc.* **2005**, *127*, 13154–13155. [[CrossRef](#)]
35. Nadres, E.T.; Santos, G.I.F.; Shabashov, D.; Daugulis, O. Scope and limitations of auxiliary-assisted, palladium-catalyzed arylation and alkylation of sp^2 and sp^3 C–H bonds. *J. Org. Chem.* **2013**, *78*, 9689–9714. [[CrossRef](#)]
36. Gates, D.P.; Svejda, S.A.; Oñate, E.; Killian, C.M.; Johnson, L.K.; White, P.S.; Brookhart, M. Synthesis of branched polyethylene using (α -diimine)nickel(II) catalysts: Influence of temperature, ethylene pressure, and ligand structure on polymer properties. *Macromolecules* **2000**, *33*, 2320–2334. [[CrossRef](#)]
37. Maldanis, R.J.; Wood, J.S.; Chandrasekaran, A.; Rausch, M.D.; Chien, J.C.W. The formation and polymerization behavior of Ni(II) α -diimine complexes using various aluminum activators. *J. Org. Chem.* **2002**, *645*, 158–167. [[CrossRef](#)]
38. Cherian, A.E.; Lobkovsky, E.B.; Coates, G.W. Chiral anilines: Development of C_2 -symmetric, late-transition metal catalysts for isoselective 2-butene polymerization. *Chem. Commun.* **2003**, 2566–2567. [[CrossRef](#)]
39. Cherian, A.E.; Rose, J.M.; Lobkovsky, E.B.; Coates, G.W. A C_2 -symmetric, living α -diimine Ni(II) catalyst: Regioblock copolymers from propylene. *J. Am. Chem. Soc.* **2005**, *127*, 13770–13771. [[CrossRef](#)]
40. Vaidya, T.; Klimovica, K.; LaPointe, A.M.; Keresztes, I.; Lobkovsky, E.B.; Daugulis, O.; Coates, G.W. Secondary alkene insertion and precision chain-walking: A new route to semicrystalline “polyethylene” from α -olefins by combining two rare catalytic events. *J. Am. Chem. Soc.* **2014**, *136*, 7213–7216. [[CrossRef](#)]
41. O’Connor, K.S.; Watts, A.; Vaidya, T.; LaPointe, A.M.; Hillmyer, M.A.; Coates, G.W. Controlled chain walking for the synthesis of thermoplastic polyolefin elastomers: Synthesis, structure, and properties. *Macromolecules* **2016**, *49*, 6743–6751. [[CrossRef](#)]
42. O’Connor, K.S.; Lamb, J.R.; Vaidya, T.; Keresztes, I.; Klimovica, K.; LaPointe, A.M.; Daugulis, O.; Coates, G.W. Understanding the insertion pathways and chain walking mechanisms of α -diimine nickel catalysts for α -olefin polymerization: A ^{13}C NMR spectroscopic investigation. *Macromolecules* **2017**, *50*, 7010–7027. [[CrossRef](#)]

43. Padilla-Vélez, O.; O'Connor, K.S.; LaPointe, A.M.; MacMillan, S.N.; Coates, G.W. Switchable living nickel(II) α -diimine catalyst for ethylene polymerisation. *Chem. Commun.* **2019**, *55*, 7607–7610. [[CrossRef](#)] [[PubMed](#)]
44. Ma, X.; Zhang, Y.; Jian, Z. Tunable branching and living character in ethylene polymerization using “polyethylene glycol sandwich” α -diimine nickel catalysts. *Polym. Chem.* **2021**, *12*, 1236–1243. [[CrossRef](#)]
45. Batsanov, S.S. Van der Waals radii of elements. *Inorg. Mater.* **2001**, *37*, 871–885. [[CrossRef](#)]
46. Medina, J.T.; Tran, Q.H.; Hughes, R.P.; Wang, X.; Brookhart, M.; Daugulis, O. Ethylene polymerizations catalyzed by fluorinated “sandwich” diimine-nickel and palladium complexes. *J. Am. Chem. Soc.* **2024**, *146*, 15143–15154. [[CrossRef](#)]
47. Zheng, H.; Li, Y.; Du, W.; Cheung, C.S.; Li, D.; Gao, H.; Deng, H.; Gao, H. Unprecedented square-planar α -diimine dibromonickel complexes and their ethylene polymerizations modulated by Ni–phenyl interactions. *Macromolecules* **2022**, *55*, 3533–3540. [[CrossRef](#)]
48. Zheng, H.; Qiu, Z.; Gao, H.; Li, D.; Cheng, Z.; Tu, G.; Gao, H. Noncovalent Ni–phenyl interactions promoted α -diimine nickel-catalyzed copolymerization of ethylene and methyl acrylate. *Macromolecules* **2024**, *57*, 5279–5288. [[CrossRef](#)]
49. Falivene, L.; Cao, Z.; Petta, A.; Serra, L.; Poater, A.; Oliva, R.; Scarano, V.; Cavallo, L. Towards the online computer-aided design of catalytic pockets. *Nat. Chem.* **2019**, *11*, 872–879. [[CrossRef](#)]
50. Eagan, J.M.; Padilla-Vélez, O.; O'Connor, K.S.; MacMillan, S.N.; LaPointe, A.M.; Coates, G.W. Chain-straightening polymerization of olefins to form polar functionalized semicrystalline polyethylene. *Organometallics* **2022**, *41*, 3411–3418. [[CrossRef](#)]
51. Lu, W.; Liao, Y.; Dai, S. Facile access to ultra-highly branched polyethylenes using hybrid “sandwich” Ni(II) and Pd(II) catalysts. *J. Catal.* **2022**, *411*, 54–61. [[CrossRef](#)]
52. Dai, S.; Li, S. Effect of aryl orientation on olefin polymerization in iminopyridyl catalytic system. *Polymer* **2020**, *200*, 122607. [[CrossRef](#)]
53. Li, S.; Dai, S. Highly efficient incorporation of polar comonomers in copolymerizations with ethylene using iminopyridyl palladium system. *J. Catal.* **2021**, *393*, 51–59. [[CrossRef](#)]
54. Li, S.; Dai, S. 8-Arylnaphthyl substituent retarding chain transfer in insertion polymerization with unsymmetrical α -diimine systems. *Polym. Chem.* **2020**, *11*, 7199–7206. [[CrossRef](#)]
55. Dai, S.; Sui, X.; Chen, C. Synthesis of high molecular weight polyethylene using iminopyridyl nickel catalysts. *Chem. Commun.* **2016**, *52*, 9113–9116. [[CrossRef](#)]
56. Chen, Z.; Allen, K.E.; White, P.S.; Daugulis, O.; Brookhart, M. Synthesis of branched polyethylene with “half-sandwich” pyridine-imine nickel complexes. *Organometallics* **2016**, *35*, 1756–1760. [[CrossRef](#)]
57. Ge, Y.; Cai, Q.; Wang, Y.; Gao, J.; Chi, Y.; Dai, S. Synthesis of high-molecular-weight branched polyethylene using a hybrid “sandwich” pyridine-imine Ni(II) catalyst. *Front. Chem.* **2022**, *10*, 886888. [[CrossRef](#)]
58. Liao, Y.-D.; Cai, Q.; Dai, S.-Y. Synthesis of high molecular weight polyethylene and E-MA copolymers using iminopyridine Ni(II) and Pd(II) complexes containing a flexible backbone and rigid axial substituents. *Chin. J. Polym. Sci.* **2023**, *41*, 233–239. [[CrossRef](#)]
59. Cheng, Z.; Gao, H.; Qiu, Z.; Zheng, H.; Li, D.; Jiang, L.; Gao, H. π – π Interactions-driven ethylene polymerization using “sandwich” bis(imino)pyridyl iron catalysts. *ACS Catal.* **2024**, *14*, 7956–7966. [[CrossRef](#)]
60. Chen, Z.; Mesgar, M.; White, P.S.; Daugulis, O.; Brookhart, M. Synthesis of branched ultrahigh-molecular-weight polyethylene using highly active neutral, single-component Ni(II) catalysts. *ACS Catal.* **2015**, *5*, 631–636. [[CrossRef](#)]
61. Ji, P.; Guo, L.; Hu, X.; Li, W. Ethylene polymerization by salicylaldimine nickel(II) complexes derived from aryl naphthylamine. *J. Polym. Res.* **2017**, *24*, 30. [[CrossRef](#)]
62. Kenyon, P.; Wörner, M.; Mecking, S. Controlled polymerization in polar solvents to ultrahigh molecular weight polyethylene. *J. Am. Chem. Soc.* **2018**, *140*, 6685–6689. [[CrossRef](#)] [[PubMed](#)]
63. Wang, C.; Kang, X.; Mu, H.; Jian, Z. Positive effect of polar solvents in olefin polymerization catalysis. *Macromolecules* **2022**, *55*, 5441–5447. [[CrossRef](#)]
64. Zou, C.; Dai, S.; Chen, C. Ethylene polymerization and copolymerization using nickel 2-iminopyridine-n-oxide catalysts: Modulation of polymer molecular weights and molecular-weight distributions. *Macromolecules* **2018**, *51*, 49–56. [[CrossRef](#)]
65. Tran, Q.H.; Brookhart, M.; Daugulis, O. New neutral nickel and palladium sandwich catalysts: Synthesis of ultra-high molecular weight polyethylene (UHMWPE) via highly controlled polymerization and mechanistic studies of chain propagation. *J. Am. Chem. Soc.* **2020**, *142*, 7198–7206. [[CrossRef](#)]
66. Liang, T.; Goudari, S.B.; Chen, C. A simple and versatile nickel platform for the generation of branched high molecular weight polyolefins. *Nat. Commun.* **2020**, *11*, 372. [[CrossRef](#)]
67. Small, B.L.; Brookhart, M.; Bennett, A.M.A. Highly active iron and cobalt catalysts for the polymerization of ethylene. *J. Am. Chem. Soc.* **1998**, *120*, 4049–4050. [[CrossRef](#)]
68. Britovsek, G.J.P.; Gibson, V.C.; McTavish, S.J.; Solan, G.A.; White, A.J.P.; Williams, D.J.; Britovsek, G.J.P.; Kimberley, B.S.; Maddox, P.J. Novel olefin polymerization catalysts based on iron and cobalt. *Chem. Commun.* **1998**, 849–850. [[CrossRef](#)]
69. Gibson, V.C.; Redshaw, C.; Solan, G.A. Bis(imino)pyridines: Surprisingly reactive ligands and a gateway to new families of catalysts. *Chem. Rev.* **2007**, *107*, 1745–1776. [[CrossRef](#)]
70. Yu, J.; Liu, H.; Zhang, W.; Hao, X.; Sun, W.-H. Access to highly active and thermally stable iron precatalysts using bulky 2-[1-(2,6-dibenzhydryl-4-methylphenylimino)ethyl]-6-[1-(arylimino)ethyl]pyridine ligands. *Chem. Commun.* **2011**, *47*, 3257–3259. [[CrossRef](#)]

71. Mitchell, N.E.; Anderson, W.C., Jr.; Long, B.K. Mitigating chain-transfer and enhancing the thermal stability of co-based olefin polymerization catalysts through sterically demanding ligands. *J. Polym. Sci. Part A Polym. Chem.* **2017**, *55*, 3990–3995. [[CrossRef](#)]
72. Schnitte, M.; Scholliers, J.S.; Riedmiller, K.; Mecking, S. Remote perfluoroalkyl substituents are key to living aqueous ethylene polymerization. *Angew. Chem. Int. Ed.* **2020**, *59*, 3258–3263. [[CrossRef](#)] [[PubMed](#)]
73. Wang, B.; Daugulis, O.; Brookhart, M. Ethylene polymerization with Ni(II) diimine complexes generated from 8-halo-1-naphthylamines: The role of equilibrating Syn/Anti diastereomers in determining polymer properties. *Organometallics* **2019**, *38*, 4658–4668. [[CrossRef](#)]
74. Ge, Y.; Li, S.; Fan, W.; Dai, S. Flexible “sandwich” (8-alkylnaphthyl α -diimine) catalysts in insertion polymerization. *Inorg. Chem.* **2021**, *60*, 5673–5681. [[CrossRef](#)] [[PubMed](#)]
75. Ge, Y.; Lu, Z.; Dai, S. Flexible axial shielding strategy for the synthesis of high-molecular-weight polyethylene and polar functionalized polyethylene with pyridine-imine Ni(II) and Pd(II) complexes. *Organometallics* **2022**, *41*, 2042–2049. [[CrossRef](#)]
76. Klimovica, K.; Kirschbaum, K.; Daugulis, O. Synthesis and properties of “sandwich” diimine-coinage metal ethylene complexes. *Organometallics* **2016**, *35*, 2938–2943. [[CrossRef](#)]
77. Liu, C.; Shen, H.-Q.; Chen, M.-W.; Zhou, Y.-G. C₂-Symmetric hindered “sandwich” chiral N-heterocyclic carbene precursors and their transition metal complexes: Expedient syntheses, structural authentication, and catalytic properties. *Organometallics* **2018**, *37*, 3756–3769. [[CrossRef](#)]
78. Hubbell, A.K.; Lamb, J.R.; Klimovica, K.; Mulzer, M.; Shaffer, T.D.; MacMillan, S.N.; Coates, G.W. Catalyst-controlled regioselective carbonylation of isobutylene oxide to pivalolactone. *ACS Catal.* **2020**, *10*, 12537–12543. [[CrossRef](#)]
79. Klimovica, K.; Heidlas, J.X.; Romero, I.; Le, T.V.; Daugulis, O. “Sandwich” diimine-copper catalysts for C–H functionalization by carbene insertion. *Angew. Chem. Int. Ed.* **2022**, *61*, e202200334. [[CrossRef](#)]
80. Le, T.V.; Romero, I.; Daugulis, O. “Sandwich” diimine-copper catalyzed trifluoroethylation and pentafluoropropylation of unactivated C(sp³)-H bonds by carbene insertion. *Chem. Eur. J.* **2023**, *29*, e202301672. [[CrossRef](#)]

Disclaimer/Publisher’s Note: The statements, opinions and data contained in all publications are solely those of the individual author(s) and contributor(s) and not of MDPI and/or the editor(s). MDPI and/or the editor(s) disclaim responsibility for any injury to people or property resulting from any ideas, methods, instructions or products referred to in the content.